3-D Printed All-Dielectric Dual-Band Broadband Reflectarray with a Large Frequency-Ratio

Jianfeng Zhu, *Student Member, IEEE*, Yang Yang, *Senior Member, IEEE,* David McGloin, and Shaowei Liao, *Senior Member, IEEE,* Quan Xue, *Fellow, IEEE*

***Abstract*—This communication proposes a new all-dielectric broadband dual-band reflectarray with a large frequency-ratio using low-cost 3-D printing. In contrast to conventional reflectarrays using metallic resonant cells or dielectric slabs as phasing elements with full metal ground, the proposed design uses air as the phasing element and a stepped dielectric mirror structure as the ground. In this way, the metal ground is removed, which makes the design an all-dielectric one. Taking advantage of the dielectric mirror that only exhibits a bandgap in the pre-designed band while allowing electromagnetic (EM) waves to pass through it at the frequency out of the bandgap region, a dual-band reflectarray is obtained. By properly selecting the bandgap frequency of the dielectric mirror, the dual-band frequency-ratio is scalable and can be very large. Furthermore, instead of using a metallic or dielectric resonator based on resonance, air layers with linear phase response are adopted as the phasing element. Thus, the reflectarray shows broadband and stable performance over the dual-band. Compared with state-of-art works using printed-circuit-boards (PCBs) or micro-fabrication, the proposed design is low-cost and lightweight, and can be rapidly prototyped. For proof-of-concept, a prototype operating at K band and V band with a frequency-ratio of 2.7 is printed and measured.**

***Index Terms*—3D printing, reflectarray, millimeter-wave (mm-wave), dual-band, frequency-ratio, dielectric mirror.**

I. Introduction

Combining many favorable features of both reflector antennas and printed antenna arrays, a reflectarray is a light-weight and low-profile high gain antenna [1-3]. The reflection phase of each pixel on the aperture can be directly controlled without a feeding network, which makes it attractive for wireless communication [4-6]. As future systems are now exploiting a wide frequency spectrum from sub-6-GHz to the low terahertz (THz) region, dual-band/multi-band reflectarrays with a large frequency ratio are becoming more and more popular [7-11]. To achieve a large frequency ratio, one approach is to utilize a stack of two phasing element layers with each operating at one frequency band. For example, a microstrip concentric dual split-loop element operating at K-band is put on the top of an L-band element [9] with frequency-selective-surface (FSS) as a spacer. Because of the stacked layers, blockage effects degrade the efficiency and gain of the lower reflectarray. To get around this problem, Deng, *et.al* proposed the Phoenix element [12] to realize a single-layer dual-band reflectarray, albeit with a restricted frequency-ratio of up to 2. Dielectric-based reflectarrays are also widely used to avoid conductor loss since the loss in the resonant metallic phasing elements increases to a degree at THz frequencies and above [13]. For example, dielectric slabs with variable heights are commonly used as the phasing element [14-21]. Nevertheless, these designs operate at a single frequency band because the dielectric slabs can only achieve a 2π phase change over one frequency band. In the THz and optical bands, many reported reflectarrays present low loss using high dielectric materials (such as high-resistivity silicon (HR Si) and titanium dioxide) as dielectric resonators (DR) sitting on a gold ground [22-24]. Currently, most dielectric-based reflectarrays are constructed from dielectric slabs (perforated holes), or DR as the phasing element and metal plane as ground. To the best of our knowledge, an all-dielectric dual-band reflectarray with a large frequency-ratio has not been previously reported.

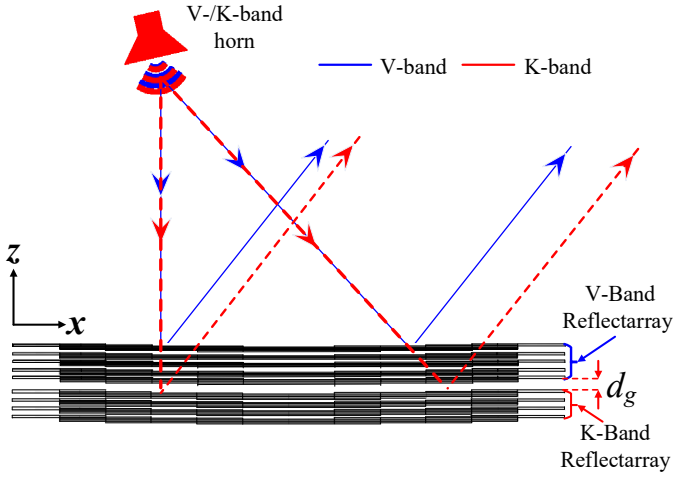

Fig. 1. Configuration of the proposed dual-band all-dielectric reflectarray. (dg=4.8 mm).

3-D printing, also known as additive manufacturing, has provided a new and economical way to construct low-cost beam shaping devices compared to subtractive microfabrication techniques [25]. More importantly, 3-D printing is good at processing complicated structures, which is difficult to achieve in traditional fabrication. Many dielectric-based devices operating from microwave to THz regions have been demonstrated with good performance and low cost using 3-D printing, such as lenses [26-31], phase plates [32] and Bessel beam launchers [33].

In this communication, we propose an all-dielectric dual-band reflectarray that adopts a stepped dielectric mirror as the ground and air as the phasing element. In this way, the conventional metal ground is removed and enables 3D printing of the whole device. Unlike a full metal ground, a dielectric mirror only has bandgap characteristics at the pre-designed frequency. Out of the bandgap, electromagnetic (EM) waves can pass through it with little hindrance. This feature makes the dual-band property of the dielectric-based reflectarray possible. By properly selecting the bandgap feature of the dielectric mirror, the dual-band frequency-ratio is scalable and can be very large. Furthermore, since phase tuning is realized using an air layer with a

Manuscript received XX, 2020. This work was fully funded by Blue Sky Grant, Tech Lab, Faculty of Engineering and Information Technology, University of Technology Sydney. (Corresponding author: Yang Yang yang.yang.au@ieee.org; yang.yang-1@uts.edu.au)

Jianfeng Zhu, Yang Yang and David McGloin are with school of Electrical and Data Engineering, University of Technology Sydney, Ultimo, NSW 2007, Australia (e-mail: zhujianfeng@ieee.org, yang.yang.au@ieee.org)

Shaowei Liao and Quan Xue are with the School of Electronic and Information Engineering, South China University of Technology, Guangzhou 510006, China.

linear phase response, the reflectarray is broadband and shows stable performance. Besides, no mutual interference occurs between the dual-band in regard to phase, and thus the compensating phase of the dual bands can be considered independently. A prototype operating at K band and V band is printed and measured to verify the idea.

II. Dual-Band All-Dielectric Reflectarray

We take the design of a K-/V-band reflectarray as an example to illustrate the idea. The basic configuration of the proposed dual-band all-dielectric reflectarray is shown in Fig. 1. The high-band reflectarray is on the top, which can reflect and collimate the EM-wave at V-band and allow the K-band EM-wave to pass. The bottom reflectarray reflects and collimates the K-band wave.

A. Dielectric Mirror

The basic building block of the reflectarray is based on the dielectric mirror, which is formed by periodically stacking dielectric layers and air layers, as shown in Fig. 2 (a). At low frequencies, i.e. the wavelength is much longer than the periodicity, the wave propagates through the structure as if the structure is homogenous with the corresponding effective refractive index. As the frequency increases, multiple partial reflections from the boundaries (between two materials with different refractive indexes) become important and all these partially reflected waves interfere with each other and give rise to a significant overall reflection. Eventually, when the cut-off frequency is reached, the wave is completely reflected. This cut-off frequency and the bandgap can be found using eigenmode analysis in ANSYS HFSS assuming infinite periodicities, as shown in Fig. 2 (b) and (c).

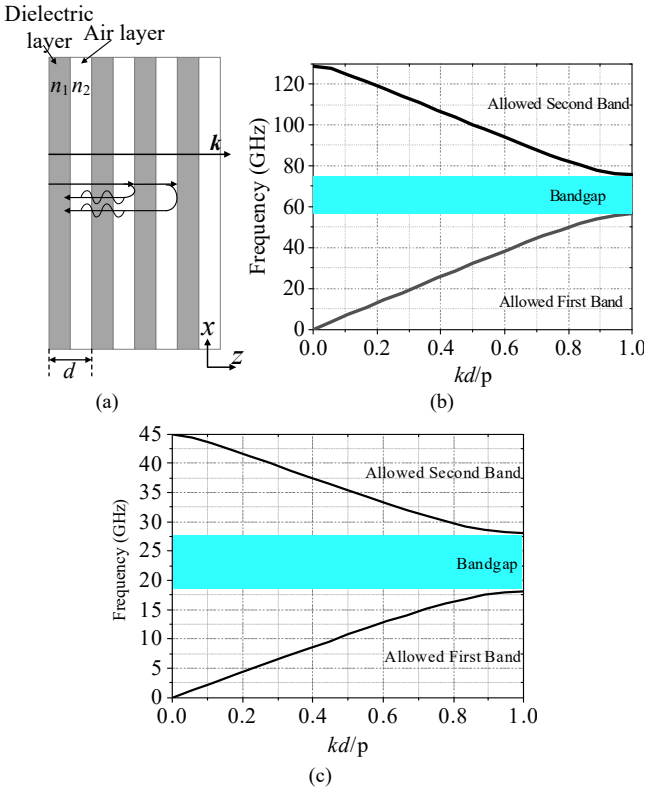

Fig. 2 (a) Basic configuration of the dielectric mirror. (k is propagation constant inside medium). (b) Dispersion curve of the proposed V-band dielectric mirror structure. (c) Dispersion curve of the proposed K-band dielectric mirror structure.

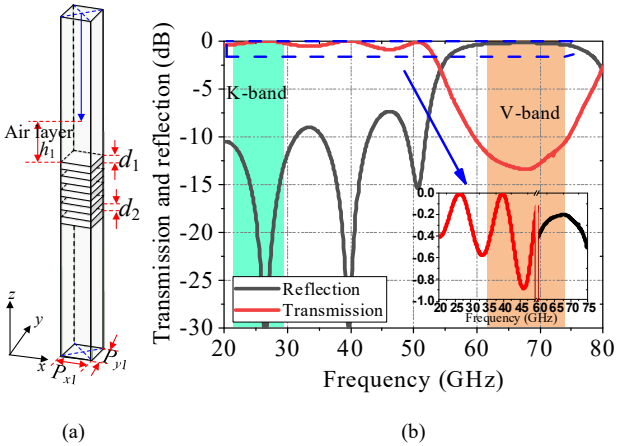

Fig. 3. (a) Simulation model of dielectric mirror in ANSYS HFSS for V-band reflectarray. (b) Transmission and reflection coefficients of the structure. (d_1=0.8 mm, d_2=1 mm, P_{x1}=P_{y1}=3.5 mm).

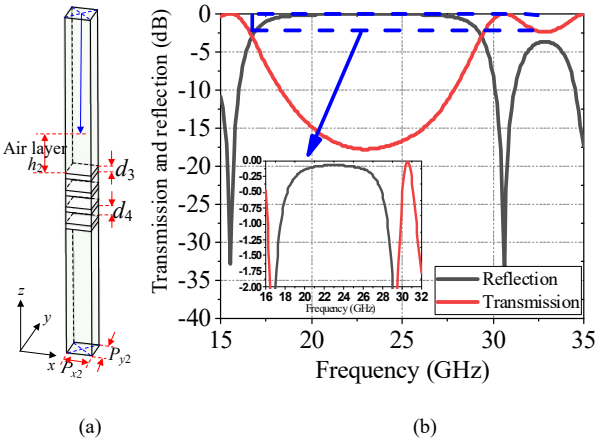

Fig. 4. (a) Simulation model of dielectric mirror structure in ANSYS HFSS for K-band reflectarray. (b) Transmission and reflection coefficients of the structure. (d_3=1.5 mm, d_4=3.5 mm, P_{x2}=P_{y2}=7.5 mm).

Note that multiple bandgaps can be achieved using the periodical structure, but only the lowest bandgap is used in the design. The location of the bandgap can be adjusted by tuning the length of the periodicity. The larger the periodicity is, the lower frequency of the first bandgap will be. This means one can easily control the bandgap of the dielectric mirror and thus the operating frequencies of the reflectarray. The bandwidth of the bandgap can also be controlled as the bandgap region increase with the index difference (n_1-n_2) [34].

Ideally, the dielectric stack of the dielectric mirror is infinite. In practice, sufficient reflection can be achieved by using multiple periodicities of the dielectric stack. In the design, the reflectarray in the high-band is achieved by stacking five-dielectric layers using polylactic acid (PLA) with a dielectric constant of 2.5, loss tangent of 0.025, and thickness of 0.8 mm in order. The distance between two adjacent dielectric layers (air layer) is 1 mm. The lower-band reflectarray stacks four-dielectric layers (PREPERM® 3-D ABS) with a dielectric constant of 4, loss tangent of 0.004, and a thickness of 1.5 mm. The distance between two adjacent dielectric layers is 3.5 mm. The simulation model of the V-band dielectric mirror structure and its corresponding transmission and reflection coefficients are shown in

Fig. 3. From 60 GHz to 75 GHz (bandgap region), the reflection coefficient is near 0 dB while the reflection coefficient is lower than -

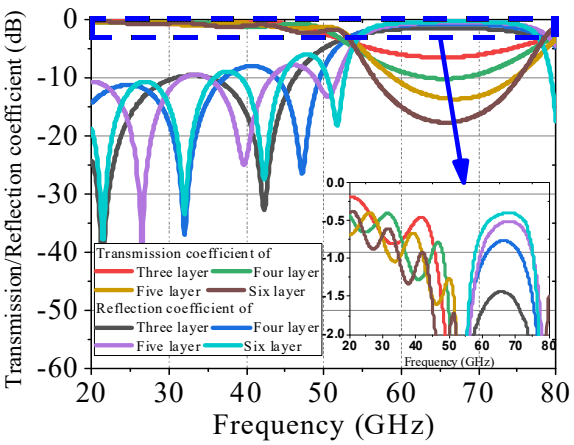

(a)

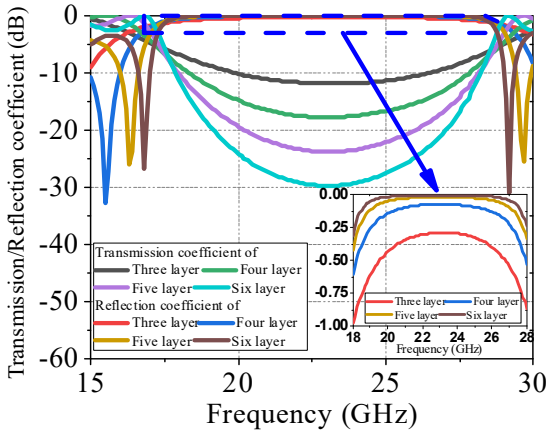

(b)

Fig.5. (a) Simulation transmission/reflection coefficients of dielectric mirror for V-band reflectarray with different dielectric layers. (b) Simulation transmission/reflection coefficients of dielectric mirror for K-band reflectarray with different dielectric layers.

10 dB from 20 GHz to 30 GHz, indicating V-band reflection and K-band transmission. The K-band dielectric mirror structure and its corresponding transmission and reflection coefficients are shown in Fig. 4. From 18 GHz to 27.5 GHz, the reflection coefficient is also near 0 dB, demonstrating the EM-wave is reflected by the dielectric mirror at the K band.

The transmission/reflection coefficients of the V-band and K-band dielectric mirror structure with different layers are given in Fig. 5. It is observed that better reflection can be achieved if more layers are used. Nevertheless. the thickness of the reflectarray is increased as well. Therefore, the number of layers is determined based on the trade-off between the good reflection and the thickness of the reflectarray. In the proposed design, five layers and four layers are adopted for the V-band and K-band, respectively. The transmission coefficients of the two structures are lower than -13 dB and -17 dB, respectively, which show sufficient reflection to form the dielectric mirror.

As the dielectric mirror structures are used for the building blocks of the reflectarray, it is important to investigate the performance of the dielectric mirror structures under oblique incident waves. The simulated reflection coefficients of the dielectric mirror structures

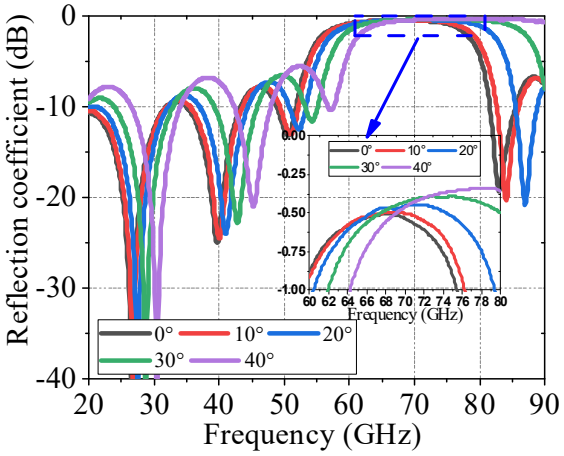

(a)

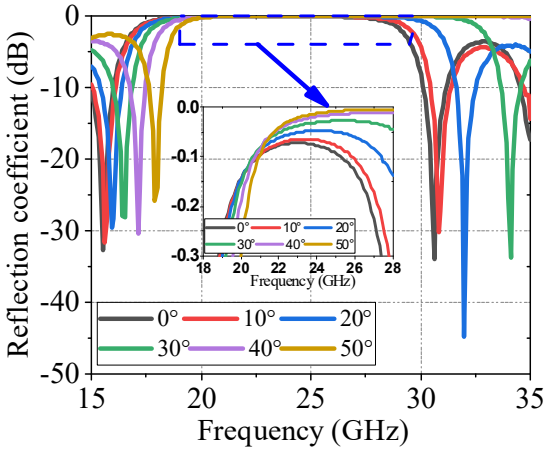

(b)

Fig. 6. (a) The reflection coefficients of V-band dielectric mirror structure under oblique incident angles. (b) The reflection coefficients of the K-band dielectric mirror structure under oblique incident angles.

under incident angle up to 40-degree are shown in Fig. 5. It is found that the bandgaps of the V band and K band are very stable and the operating bandgaps slightly shift to the higher frequency when the incident angle increases.

B. Reflectarray Design

The array of the proposed dielectric mirror structure in Section II. A is built in a stepped configuration to form the reflectarray. In this way, the air is used as the wideband phasing element, which is different from conventional designs using dielectric slabs [17-20]. The reflectarray is synthesized using eight unit cells (UCs) (3-bit phase quantization). Therefore, the thicknesses of the air layer (h_1) for V-band are 0 mm, 0.288mm, 0.576 mm, 0.864mm, 1.152 mm, 1.44 mm, 1.728 mm, 2.016 mm, and their corresponding reflection phases are given in Fig. 7 (a). The thicknesses of the air layer (h_2) for K-band are 0 mm, 0.78mm, 1.56 mm, 2.34 mm, 3.12 mm, 3.9 mm, 4.68 mm, 5.46 mm, and their corresponding reflection phases are given in Fig. 7 (b). Nearly linearly phase response can be observed in both bands. The phase compensation on the aperture is calculated according to Fermat's principle of equality of electrical path lengths of incoming EM waves [3]:

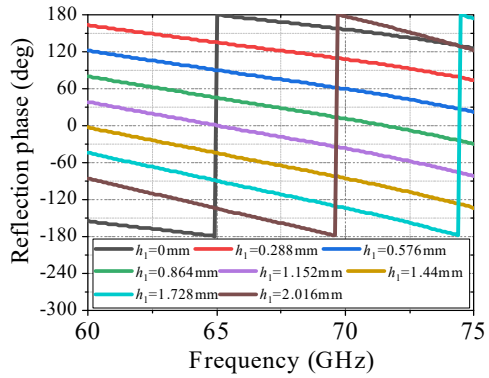

(a)

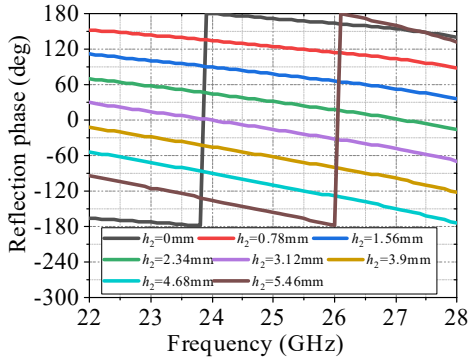

(b)

Fig.7. (a) Reflection phase of eight UC at V-band. (b) Reflection phase of eight UC at K-band.

$$\varphi(x,y)=\frac{2\pi}{\lambda_0}\left(\sqrt{x^2+y^2+f^2}-f\right)+\varphi_0 \tag{1}$$

where f is the focal length, λ_0 represents free-space wavelength and φ_0 is the initial phase at the original point. The aperture size is 77 mm × 77 mm and the focal length is set as 150 mm. 22 × 22 and 10 × 10 sets of phasing elements are used for the high-band and low-band reflectarray, respectively. Generally, for conventional multi-layered reflectarrays, the upper phasing element will affect the bottom phasing element due to mutual coupling. A high-performance FSS structure has to be used to avoid such coupling [8],[9]. In the proposed design, because all the phasing elements of the upper reflectarray are the same (only positions along the z-direction are different), they do not impose change on the compensating phase of the lower reflectarray. Thus, the compensating phase of the two bands can be considered independently.

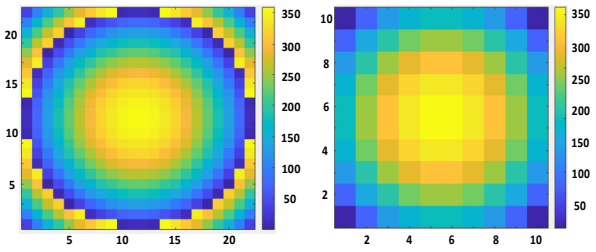

(a) (b)

Fig. 8. (a) Compensating phase at V band. (b) Compensating phase at the K band.

The calculated compensating phase masks of the high-band and low-band reflectarray are shown in Fig. 8.

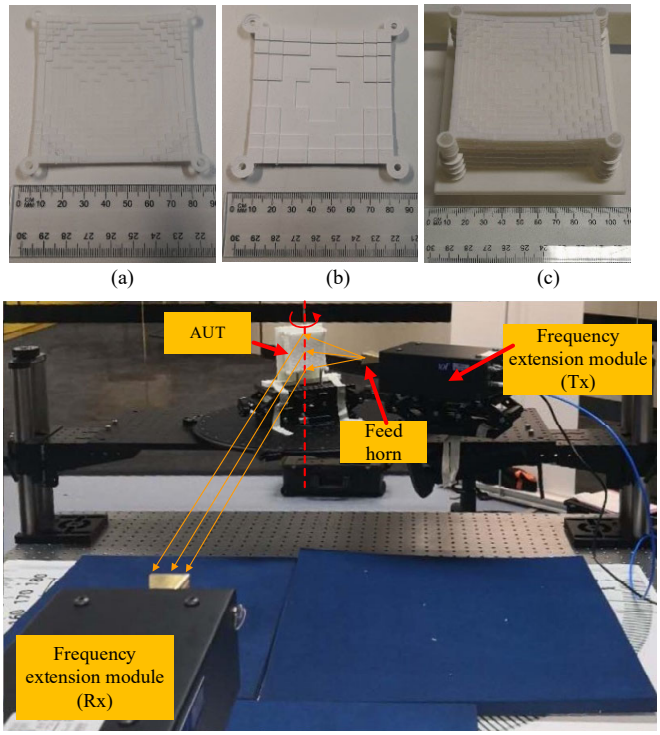

(a) (b) (c)

(d)

Fig. 9. (a) Top view of the V-band structure. (b) Top view of the K-band structure. (c) Assembled view. (d) Measurement system.

III. Fabrication and Measurement

The prototype of the reflectarray is fabricated using a generic 3-D printer, a Flashforge Guider II, as shown in Figs. 9 (a)-(b). The V-band/K-band reflectarrays are composed of five/four dielectric layers,

TABLE I

Comparison of Different Dual-Band Reflectarrays

Ref	Configurations	Operating Frequency	Mutual interference	Gain	Frequency ratio	Fabrication
[7]	Single layer phasing element + full Ground	29.8/20	Strong	40/35.8	1.49	PCB
[8]	Multi-layer phasing element + FSS	30.2/20.4	Weak	40.2/36.7	1.48	PCB
[9]	Multi-layer phasing element + FSS	9.8/20	Medium	38.5/36.4 (directivity)	1.49	PCB
[10]	Single-layer phasing element + full Ground	30/20	Medium	38.9/36.7	1.5	PCB
[11]	Multi-layer phasing element	29.7/19.7	Strong	38.5/35.1 (directivity)	1.5	PCB
[12]	Single layer phasing element + full Ground	20/10	Weak	36.1/30.3	2	PCB
[35]	Single layer phasing element + full Ground	13.5/9	Weak	23.4/17.8	1.5	PCB
[36]	DR+ full ground	10/5.68	Weak	23/19	1.76	N.A.
This work	Dielectric mirror + air	65/24	Weak	30.7/23.2	2.7	3-D printing

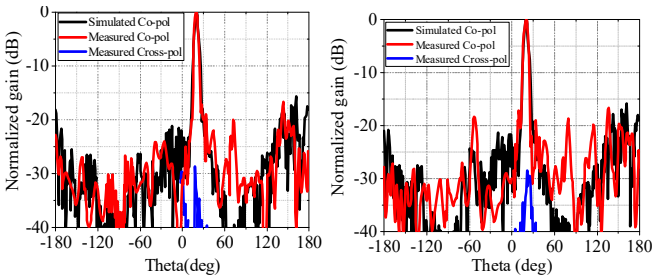

Fig. 10. Simulated and measured radiation patterns. (a) 66 GHz. (b) 70 GHz.

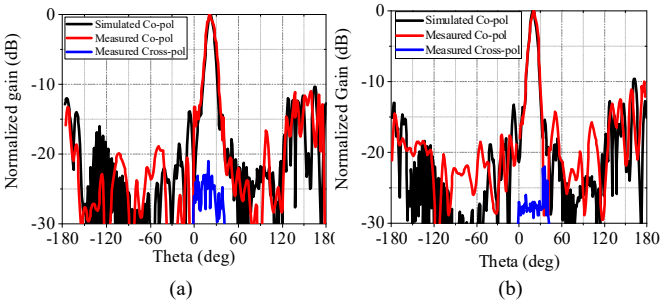

Fig. 11. Simulated and measured radiation patterns. (a) 24 GHz. (b) 27 GHz.

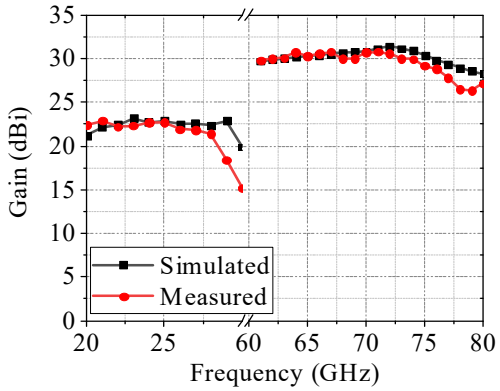

Fig. 12. Simulated and measured antenna gain.

respectively, and then they are assembled, as shown in Fig. 9 (c). The radiation performance is measured by using a far-field measurement system, as shown in Fig. 9 (d). The gain of the V-band feed horn is 20 dBi at 65 GHz and the gain of the K-band feed horn is 21.05 at 24-GHz. To reduce the blocking effect, the inclination angle of the feed horn antenna is offset by -20-degree, and thus the reflection direction is 20°. The radiation patterns at the V band (66-GHz & 70-GHz) and K band (24 GHz&27-GHz) are shown in Figs. 10 and 11, respectively. The measured gains are shown in Fig. 12. The peak gain is 30.7 dBi for the V band and 23.2 dBi for the K band. Because air is used as phasing elements with linear phase response, the reflectarray shows broadband performance with a 1-dB gain bandwidth of 32% (from 21 to 29 GHz) for the K band and 15.7% (from 64 to 75 GHz) for the V band.

IV. Discussion

Table I compares the proposed reflectarray with previous devices. As can be seen, most of the dual-band reflectarray antennas are based on metallic resonators either printed in a single layer or arranged in multiple layers. Additional efforts are required to reduce the mutual coupling between different resonant cells, such as using FSS or designing sophisticated resonators [8-10]. In [36], a dual-band dielectric reflectarray was proposed by cutting a notch on the dielectric resonator, which remains complicated to fabricate. Additionally, because the metallic structure and DR are based on resonance, the bandwidths of the designs are generally narrow. In fact, existing dielectric-based reflectarrays are always implemented by planting dielectric slabs or DR on a full metal ground. While for the proposed design, no metal is required, making the design all-dielectric. Since the 2π phase shift is achieved not based on resonance, the reflectarray can achieve broadband and stable performance over a dual-band. Considering the resolution/fabrication tolerance of the FDM-based 3D printing, we choose the periods of the unit cell (UC) as 3.5 mm (0.76 λ0@ 65GHz) and 7.5mm (0.6 λ0@ 24GHz). A smaller UC period can be used for better phase compensation. However, there is a trade-off between the reflectarray performance and fabrication resolution/tolerance. Since the all-dielectric reflectarray does not rely on UC resonance, we choose to use relatively bigger UC sizes for easy fabrication.

Because the dielectric mirror structure is isotropic, the design concept is also useful for circularly polarized EM-wave. The dielectric mirror structure is more suitable for building a large frequency ratio reflectarray regarding the frequency ratio. A dielectric mirror structure with higher frequency selectivity and better out-of-band transmission should be used for a small frequency ratio. It is also worth mentioning that, during the printing process, we found that the PLA-based dielectric mirror shows better surface roughness and mechanical performance than the ABS-based one. For this reason, we adopted PLA to form the V-band dielectric mirror, albeit a higher loss tangent.

V. Conclusion

In summary, a 3-D printed dual-band dielectric-only reflectarray operating at V band and K band is proposed and demonstrated. Taking advantage of the dielectric mirror that only exhibits a bandgap in the pre-designed band while allowing EM waves to pass through it at the frequency out of the bandgap region, a dual-band reflectarray is obtained. The Air layer is used as the phasing element, enabling an all-dielectric reflectarray with broadband feature over two bands. Because of independent phase control, the dual-band frequency-ratio can be very large. Besides, the design enjoys the benefit of 3-D printing at low-cost and lightweight.

Reference

[1] J. Huang and J. A. Encinar, *Reflectarray Antennas*. New York, NY, USA: Wiley, 2008.
[2] F. Yang and Y. Rahmat-Samii, Eds., *Surface Electromagnetics: With Applications in Antenna, Microwave, and Optical Engineering*. Cambridge, U.K.: Cambridge Univ. Press, 2019.
[3] P. Nayeri, F. Yang, and A. Z. Elsherbeni, *Reflectarray Antennas: Theory, Designs, and Applications*. Hoboken, NJ, USA: Wiley, 2018.
[4] B. Evans, *Satellite Communication Systems*. London, U.K.: Inst. Eng. Technol., 1999.
[5] P. Nayeri, F. Yang, and A. Elsherbeni, "Beam scanning reflectarray antennas: A technical overview and state of the art," *IEEE Antennas Propag. Mag.*, vol. 57, no. 4, pp. 32–47, Aug. 2015.
[6] R. Florencio, J. A. Encinar, R. R. Boix, V. Losada, and G. Toso, "Reflectarray antennas for dual polarization and broadband telecom satellite applications," *IEEE Trans. Antennas Propag.*, vol. 63, no. 4, pp. 1234– 1246, Apr. 2015.
[7] T. Smith, U. Gothelf, O. S. Kim, and O. Breinbjerg, "Design, manufacturing, and testing of a 20/30-GHz dual-band circularly polarized

reflectarray antenna," *IEEE Antennas Wireless Propag. Lett*., vol. 12, pp. 1480–1483, Nov. 2013.

[8] R. Deng, F. Yang, S. Xu and M. Li, "An FSS-Backed 20/30-GHz dual-band circularly polarized reflectarray with suppressed mutual coupling and enhanced performance," *IEEE Trans. Antennas Propag,* vol. 65, no. 2, pp. 926-931, Feb. 2017.

[9] T. Smith, U. Gothelf, O. S. Kim, and O. Breinbjerg, "An FSS backed 20/30 GHz circularly polarized reflectarray for a shared apertureL- and Ka-band satellite communication antenna," *IEEE Trans. Antennas Propag*., vol. 62, no. 2, pp. 661–668, Feb. 2014.

[10] R. Deng, Y. Mao, S. Xu and F. Yang, "A single-layer dual-band circularly polarized reflectarray with high aperture efficiency," *IEEE Trans. Antennas Propag.*, vol. 63, no. 7, pp. 3317-3320, July 2015.

[11] J. M. Baracco, P. Ratajczak, P. Brachat, and G. Toso, "A dual frequency Ka-band printed Fresnel reflector for ground terminal applications*," IEEE Trans. Antennas Propag.,* vol. 63, no. 10, pp. 4352–4366, Oct. 2015.

[12] R. Deng, S. Xu, F. Yang and M. Li, "Single-layer dual-band reflectarray antennas with wide frequency ratios and high aperture efficiencies using phoenix elements," *IEEE Trans. Antennas Propag*, vol. 65, no. 2, pp. 612-622, Feb. 2017, doi: 10.1109/TAP.2016.2639023.

[13] R. T. Ako, A. Upadhyay, W. Withayachumnankul, M. Bhaskaran, and S. Sriram, ''Dielectrics for terahertz metasurfaces: Material selection and fabrication techniques,'' *Adv. Opt. Mater*., vol. 8, no. 3, Feb. 2020, Art. no. 1900750.

[14] P. Nayeri et al., "3D printed dielectric reflectarrays: low-Cost high-gain antennas at sub-millimeter waves," *IEEE Trans. Antennas Propag*., vol. 62, no. 4, pp. 2000-2008, April 2014.

[15] Y. He, Z. Gao, D. Jia, W. Zhang, B. Du, and Z. N. Chen, "Dielectric metamaterial-based impedance-matched elements for broadband reflectarray, " *IEEE Trans. Antennas Propag*., vol. 65, no. 12, pp. 7019–7028, Dec. 2017.

[16] M. K. T. Al-Nuaimi, Y. He and W. Hong, "Design of inhomogeneous all-dielectric electromagnetic-wave diffusive reflectarray metasurface," *IEEE Antennas Wireless Propag. Lett*, vol. 18, no. 4, pp. 732-736, April 2019.

[17] M. D. Wu et al., "Design and measurement of a 220 GHz wideband 3-D printed dielectric reflectarray," *IEEE Antennas Wireless Propag. Lett*., vol. 17, no. 11, pp. 2094-2098, Nov. 2018.

[18] F. Ahmadi, K. Forooraghi, Z. Atlasbaf and B. Virdee, "Dual linear-polarized dielectric resonator reflectarray antenna," *IEEE Antennas Wireless Propag. Lett*., vol. 12, pp. 635-638, 2013.

[19] S. Zhang, ''Three-dimensional printed millimetre wave dielectric resonator reflectarray,'' *IET Microw., Antennas Propag*., vol. 11, no. 14, pp. 2005–2009, 2017.

[20] P. Nayeri, M. Liang, R. Sabory-Garc´ıa, M. Tuo, F. Yang, M. Gehm, H. Xin, and A. Elsherbeni, "High gain dielectric reflectarray antennas for THz applications," presented at the *IEEE Antennas and Propagation Society Int. Symp*., Orlando, FL, USA, Jul. 2013.

[21] Y. Sun and K. W. Leung, "Millimeter-wave substrate-based dielectric reflectarray," *IEEE Antennas Wireless Propag. Lett*., vol. 17, no. 12, pp. 2329-2333, Dec. 2018.

[22] D. Headland *et al*., "Dielectric resonator reflectarray as high-efficiency nonuniform terahertz metasurface," *ACS Photon*., vol. 3, no. 6, pp. 1019–1026, 2016.

[23] Z. Shi, M. Khorasaninejad, Y.-W. Huang, C. Roques-Carmes, A. Y. Zhu, W. T. Chen, V. Sanjeev, Z.-W. Ding, M. Tamagnone, K. Chaudhary, R. C. Devlin, C.-W. Qiu, and F. Capasso, ''Single-layer metasurface with controllable multiwavelength functions,'' *Nano Lett*., vol. 18, no. 4, pp. 2420–2427, Feb. 2018.

[24] W. Chen, et al. "A broadband achromatic polarization-insensitive metalens consisting of anisotropic nanostructures," Nature communications, 2019, 10(1): 1-7.

[25] B. Zhang, Y. X. Guo, H. Zirath, and Y. P. Zhang, "Investigation on 3-D-printing technologies for millimeter-wave and terahertz applications," *Proc. IEEE*, vol. 105, no. 4, pp. 723–736, Apr. 2017.

[26] K. X. Wang and H. Wong, "A wideband millimeter-wave circularly polarized antenna with 3-D printed polarizer," *IEEE Trans. Antennas Propag.*, vol. 65, no. 3, pp. 1038–1046, Mar. 2017.

[27] J. Zhu, Y. Yang, D. McGloin, R. Rajasekharan Unnithan, S. Li, S. Liao, and Q. Xue, ''3-D printed planar dielectric linear-to-circular polarization conversion and beam-shaping lenses using coding polarizer,'' *IEEE Trans. Antennas Propag*., vol. 68, no. 6, pp. 4332–4343, Jun. 2020.

[28] C. Ding and K. Luk, "A wideband high-gain circularly-polarized antenna using artificial anisotropic polarizer," *IEEE Trans. Antennas Propag*., vol. 67, no. 10, pp. 6645–6649, Oct. 2019.

[29] G. B. Wu, Y.-S. Zeng, K. F. Chan, S.-W. Qu, and C. H. Chan, "Highgain circularly polarized lens antenna for terahertz applications," *IEEE Antennas Wireless Propag. Lett*., vol. 18, no. 5, pp. 921–925, May 2019.

[30] B. Zhang, L. Wu, Y. Zhou, Y. Yang, H. Zhu, F. Cheng, Q. Chen, and K. Huang, ''A K-band 3-D printed focal-shifted twodimensional beam-scanning lens antenna with nonuniform feed,'' *IEEE Antennas Wireless Propag. Lett*., vol. 18, no. 12, pp. 2721–2725, Dec. 2019.

[31] B. Zhang *et al*., "A two-dimensional multibeam lens antenna for hydrologic radar application," *IEEE Antennas Wireless Propag. Lett*., vol. 18, no. 12, pp. 2488-2492, Dec. 2019.

[32] L. Niu, C. Liu, Q. Wu, K. Wang, Z. Yang, and J. Liu, "Generation of onedimensional terahertz Airy beam by three-dimensional printed cubicphase plate," *IEEE Photon. J*., vol. 9, no. 4, Aug. 2017, Art. no. 5900407.

[33] G.-B. Wu, K. F. Chan, S.-W. Qu, and C. H. Chan, ''A 2-D beamscanning Bessel launcher for terahertz applications,'' *IEEE Trans. Antennas Propag*., vol. 68, no. 8, pp. 5893–5903, Aug. 2020.

[34] S. O. Kasap and R. K. Sinha, *Optoelectronics and Photonics: Principles and Practices*. Upper Saddle River, NJ, USA: Prentice-Hall, 2001.

[35] S.-W. Qu, Q.-Y. Chen, M.-Y. Xia, and X. Y. Zhang, "Single-layer dual band reflectarray with single linear polarization," *IEEE Trans. Antennas Propag*., vol. 62, no. 1, pp. 199–205, Jan. 2014.

[36] M. G. N. Alsath, M. Kanagasabai, and S. Arunkumar, "Dual-band dielectric resonator reflectarray for C/X-bands," *IEEE Antennas Wireless Propag. Lett.*, vol. 11, pp. 1253–1256, 2012.